ICHEP'98 #140
Submitted to Pa 3, 5
Pl 4

DELPHI 98-125 CONF 186
22 June, 1998

Production of $K^{\pm}$, K^0, protons and Λs in $q\overline{q}$ and WW events at LEP 2

Preliminary

DELPHI Collaboration

P. Abreu [1], **A. De Angelis** [2], **R. P. Henriques** [1], **D. Liko** [2,3], **N. Neufeld** [2,3]

Abstract

The production of charged and neutral kaons, protons and Λs at centre-of-mass energies above the Z^0 peak has been studied using data taken with the DELPHI detector at LEP. The results on the average multiplicity of such identified particles and on the position ξ^* of the maximum of the $\xi_p = -\log(\frac{2p}{\sqrt{s}})$ distribution have been compared with predictions of JETSET and HERWIG, and with MLLA calculations.

Paper submitted to the ICHEP'98 Conference
Vancouver, July 22-29

[1] LIP-IST-FCUL, Av. Elias Garcia, 14-1e, P-1000 Lisboa, Portugal
[2] CERN, CH-1211 Geneva 23, Switzerland
[3] HEPHY, Osterr. Akad. d. Wissensch., Nikolsdorfergasse 18, AT-1050 Vienna, Austria

1 Introduction

The way quarks and gluons transform into hadrons is complex and not entirely understood by present theories; the most satisfactory description is given by Monte Carlo simulations. In the picture implemented in Monte Carlo simulations, the hadronization of a $q\bar{q}$ pair is split into 3 phases. In a first phase, gluon emission and parton branching of the original $q\bar{q}$ pair take place. It is believed that this phase can be described by perturbative QCD (most of the calculations have been performed in leading logarithmic approximation). In a second phase, at a certain virtuality Q_0, quarks and gluons produced in the first phase are clustered in colour singlets and transform into mesons and baryons. Only phenomenological models, which need to be tuned to the data, are available to describe this process of fragmentation; the models most frequently used in e^+e^- annihilations are based on string and cluster fragmentation. In the third phase the unstable states decay into hadrons which can be observed or identified in the detector. These models account correctly for the gross features of the $q\bar{q}$ events such as, for instance, the average multiplicity and inclusive momentum spectra up to the Z^0 energy; with LEP 2, the energy range spanned in e^+e^- interactions is doubled (up to 183 GeV), and it is interesting to check their validity.

A different and purely analytical approach (see e.g. [1] and references therein) giving quantitative predictions of hadronic spectra are QCD calculations using the so-called Modified Leading Logarithmic Approximation (MLLA) under the assumption of Local Parton Hadron Duality (LPHD) [2]. In this picture the particle yield is described by a parton cascade, and the virtuality cut-off Q_0 is lowered to values of the order of 100 MeV, comparable to the hadron masses; it is assumed that the results obtained for partons apply to hadrons as well.

The momentum spectra of particles produced can be calculated as a function of the variable ξ_p, where $\xi_p = -\log(\frac{2\mathrm{p}}{\sqrt{\mathrm{s}}})$ (p is the momentum of the particle and $\sqrt{s}$ is the centre of mass energy):

$$\frac{1}{\sigma}\frac{d\sigma}{d\xi_p} = K_{LPHD} \cdot f(\xi_p, X, \lambda) \tag{1}$$

with

$$X = \log\frac{\sqrt{\mathrm{s}}}{\mathrm{Q}_0} \quad ; \quad \lambda = \log\frac{\mathrm{Q}_0}{\Lambda_{\mathrm{eff}}} \,. \tag{2}$$

These MLLA+LPHD predictions involve three parameters: an effective scale parameter Λ_{eff}, a momentum cut-off Q_0 in the evolution of the parton cascade and an overall normalization factor K_{LPHD}. The function 1 has the form of a "humped-backed plateau", which is approximately Gaussian in ξ_p [3]. It can be approximated by a distorted Gaussian over the entire spectrum, as proposed in [4, 5]:

$$D(N, <\xi_p>, \sigma, \delta, s, k) = \frac{N}{\sigma\sqrt{2\pi}}\ \exp(\frac{1}{8}k - \frac{1}{2}s\delta - \frac{1}{4}(2+k)\delta^2 + \frac{1}{6}s\delta^3 + \frac{1}{24}k\delta^4) \tag{3}$$

where N is the average multiplicity, $\delta = \frac{\xi_p - <\xi_p>}{\sigma}$ with $<\xi_p>$ being the mean of the ξ_p distribution ($<\xi_p>$ coincides with the peak position up to the next-to-leading order only [1]), σ is the width, s the skewness and k the kurtosis of the distribution. For a pure Gaussian s and k vanish.

To check the validity of the MLLA+LPHD approach, it is interesting to study the evolution with the centre of mass energy of the maximum, ξ^*, of the ξ_p distribution. In the framework of the MLLA+LPHD the dependence of ξ^* on the centre of mass energy can be expressed as [1, 4, 6]:

$$\xi^* = Y\left(\frac{1}{2} + \sqrt{C/Y} - C/Y\right) + F_h(\lambda), \tag{4}$$

where

$$Y = \log\frac{\mathrm{E_{beam}}}{\Lambda_{\mathrm{eff}}} \quad , \quad \mathrm{C} = \left(\frac{11\mathrm{N_c}/3 + 2\mathrm{n_f}/(3\mathrm{N_c^2})}{4\mathrm{N_c}}\right)^2 \cdot \left(\frac{\mathrm{N_c}}{11\mathrm{N_c}/3 - 2\mathrm{n_f}/3}\right),$$

with N_c being the number of colours and n_f the active number of quark flavors in the fragmentation process. $F_h(\lambda)$ depends on the hadron type through the ratio $\lambda = \log\frac{\mathrm{Q_0}}{\Lambda_{\mathrm{eff}}}$ [1]:

$$F_h(\lambda) = -1.46\lambda + 0.207\lambda^2 \pm 0.06. \tag{5}$$

In the present analysis the K^+ , K^0 , p and Λ[1] spectra in e^+e^- interactions recorded by DELPHI in the years 1995 to 1997 at energies above the Z^0 (around 133, 161, 172 and 183 GeV) were measured. W pair events, produced at an energy of 183 GeV were selected as an independent sample. The measurements were compared to the MLLA+LPHD calculations and to the JETSET 7.4 and HERWIG 5.8 model predictions which use string and cluster fragmentation respectively [7, 8].

2 Data Sample and Event Selection

The DELPHI detector and its performance are described in [9, 10]. We used in the present analysis:

(1a) 6 pb^{-1} of data at centre-of-mass energy around 130 GeV (3 pb^{-1} collected during 1995 and another 3 pb^{-1} during 1997);

(1b) 6 pb^{-1} of data at centre-of-mass energy around 136 GeV (3 pb^{-1} collected during 1995 and another 3 pb^{-1} during 1997);

(2) 9.96 pb^{-1} of data around 161 GeV (1996);

(3) 10.14 pb^{-1} of data around 172 GeV (1996);

(4) 50.15 pb^{-1} of data around 183 GeV (1997).

The samples (1a) and (1b), at 130 and 136 GeV respectively, were merged into a unique sample (1), and attributed to the centre of mass energy of 133 GeV.

A preselection of hadronic events in both samples was made, requiring at least 6 charged particles with momentum p above 400 MeV/c, angle θ with respect to the beam direction between 20° and 160°, a track length of at least 30 cm, a distance of closest approach to the interaction point less than 4 cm in the plane perpendicular to the beam axis and less than 10 cm along the beam axis, and a total energy of the charged particles

[1] Unless otherwise stated antiparticles are included as well.

$\sqrt{s}$ (GeV)	$\sigma_{qq}^{(h)}$ (pb^{-1})	$\sigma_{W^+W^-}$ (pb^{-1})
133	74	–
161	35	3
172	29	12
183	25	16

Table 1: Hadronic cross section $\sigma_{qq}^{(h)}$ for effective centre-of-mass energy $> 0.85 E_{cm}$ (from ZFITTER) compared to the W^+W^- cross section $\sigma_{W^+W^-}$.

above 0.15 times the centre-of-mass energy $\sqrt{s}$. In the calculation of the energies E, all charged particles were assumed to have the pion mass.

Charged particles were then used in the analysis if they had $p > 100$ MeV/c, a relative error on the momentum measurement $\Delta p/p < 1$, polar angle $20^\circ < \theta < 160^\circ$, a track length of at least 30 cm, and a distance of closest approach to the primary vertex smaller than 3 cm in the plane perpendicular to the beam axis and 6 cm along the beam axis.

The influence of the detector on the analysis was studied with the full DELPHI simulation program, DELSIM [10]. Events were generated with JETSET 7.4 [7], with parameters tuned to fit LEP1 data in DELPHI [11]. The particles were followed through the detailed geometry of DELPHI, giving simulated digitizations in each sub-detector. These data were processed with the same reconstruction and analysis programs as the real data.

The cross-section for $e^+e^- \rightarrow q\bar{q}(\gamma)$ above the Z^0 peak is dominated by radiative $q\bar{q}\gamma$ events; the initial state radiated photons (ISR photons) are generally aligned along the beam direction and are not detected. In order to compute the hadronic centre-of-mass energy, the method described in [12] was used. The procedure clusters the particles into two jets using the Durham algorithm [13], excluding candidate ISR photons. Assuming an ISR photon along the beam pipe if no candidate ISR photon has been detected elsewhere, the energy of the ISR photon is computed from the jet directions assuming massless kinematics. The effective centre-of-mass energy of the hadronic system, $\sqrt{s'}$, is calculated as the invariant mass of the system recoiling from the ISR photon.

The method used to obtain the hadronic centre-of-mass energy overestimates the true energy in the case of double hard radiation in the initial state. For instance, if the two ISR photons are emitted back to back, the remaining two jets may also be back to back, but with energy much smaller than the beam energy. Cutting on the total energy measured in the detector reduces the contamination from such events.

The selection of the hadronic events at the various energies, after the common pre-selection, depends on the centre of mass energy due to the different background from W^+W^- pairs (table 1). For a centre of mass energy of 183 GeV, were the largest amount of data has been collected, W^+W^- pairs have been selected independently.

2.1 Hadronic Selection at 133 GeV

Events with reconstructed hadronic centre-of-mass energy ($\sqrt{s'}$) above 122 GeV, with total energy seen in the detector above $0.15\sqrt{s}$, and with at least 7 charged particles with momentum above 100 MeV/c, were used. A total of 830 events were selected in the data (790 $q\bar{q}$ predicted by the simulation).

2.2 Hadronic Selection at 161 GeV

Events with reconstructed hadronic centre-of-mass energy ($\sqrt{s'}$) above 150 GeV, with total energy seen in the detector above $0.2\sqrt{s}$, and with at least 9 charged particles with momentum above 100 MeV/c^2, were used. A total of 326 events were selected (311 predicted by the simulation; the estimated background from W^+W^- was 14 events).

2.3 Hadronic Selection at 172 GeV

Events with reconstructed hadronic centre-of-mass energy ($\sqrt{s'}$) above 155 GeV, with total energy seen in the detector above $0.2\sqrt{s}$, with at least 10 charged particles with momentum above 100 MeV/c^2, and with narrow jet broadening[2] smaller than 0.1 were used. A total of 212 events were selected (202 predicted by the simulation; the estimated background from W^+W^- was 5 events).

2.4 Hadronic Selection at 183 GeV

Events with reconstructed hadronic centre-of-mass energy ($\sqrt{s'}$) above 160 GeV, with total energy seen in the detector above $0.2\sqrt{s}$, with at least 10 charged particles with momentum above 100 MeV/c^2, and with narrow jet broadening smaller than 0.1 were used. A total of 976 events were selected (1022 predicted by the simulation; the estimated background from W^+W^- was 51 events).

2.5 WW Event Selection at 183 GeV

Events containing a W pair were selected following the procedure described in [14]. To select events $W^+W^- \to q\bar{q}Q\bar{Q}$, jets were reconstructed using the LUCLUS jet clustering algorithm with d_{join} value of 6.5 GeV. Events with a reconstructed hadronic centre-of-mass energy ($\sqrt{s'}$) above 120 GeV and at least 4 jets with 4 particles in each jet were selected. These events were then forced in a 4 jet configuration. QCD background was reduced by selecting those events fulfilling the cut $D = (E_{min}/E_{max})\theta_{min}/(E_{max} - E_{min}) < 0.0045$, where θ_{min} is the minimum inter-jet angle and E_{max} and E_{min} are the maximum and minimum jet energy respectively. Events $W^+W^- \to q\bar{q}l\nu$ were selected by requiring the presence of a hadronic system with large invariant mass, large missing momentum pointing away from the beam pipe and either one energetic isolated charged track or a low multiplicity jet. To reduce further the QCD background contributions in the electron and tau channel a cut on the acoplanarity was applied. These criteria gave 368 $W^+W^- \to q\bar{q}Q\bar{Q}$ candidates and 211 $W^+W^- \to q\bar{q}l\nu$ candidates. (365 and 210 predicted by simulation; the estimated purity of the samples was 80 ± 2 % and 95 ± 0.3 % respectively.)

---

[2] The narrow jet broadening (B) is defined as follows. For each hemisphere $j = 1, 2$ with respect to a plane perpendicular to the thrust axis: $B_j = \frac{1}{2 \cdot p_{tot}} \sum_i p_i \cdot sin\theta_{i-T}$, where p_{tot} is the sum of the moduli of the momenta of all the particles in the j-th hemisphere, p_i is the momentum of the particle i and θ_{i-T} is the angle between the direction of the particle and the thrust line. The narrow jet broadening is the minimum between B_1 and B_2.

3 Analysis

For the measurement of K^+ and p , a tagging procedure based on the combination of the Cherenkov angle measurement in the RICH detector and the ionization energy loss (dE/dx) in the TPC was applied.

The dE/dx information was used for momenta below 0.7 GeV/c for K^+ (where no RICH information is available) and up to 1.2 GeV/c for proton identification. In the remaining momentum range the tagging was performed with the RICH measurement. The analysis is restricted to the barrel RICH region ($41° \leq \theta_{track} \leq 139°$). The RICH hadron identification was based on three standard (DELPHI-RICH) software-packages: RIBMEAN, RICFIX and NEWTAG [15]. RIBMEAN calculates an average Cherenkov angle for the liquid and the gas radiator by application of a clustering algorithm and simultaneously links a quality flag to each track passing through the RICH. RICFIX corrects the RICH data and Monte Carlo concerning detector related effects (such as slight fluctuations in pressures and refractive indices, background arising from photon feedback, crosstalk between the MWPC readout strips, δ-rays, track ionization photoelectrons, etc.). In this analysis the standard NEWTAG (RICH) selections were applied to select charged kaons and protons.

The efficiency was estimated from full detector simulation, and it is $\sim 56\%$ ($\sim 46\%$) with a purity of $\sim 75\%$ ($\sim 92\%$) for K^+ (p).

K^0 and Λ candidates were detected by their decay in flight into $\pi^+\pi^-$ and $p\pi^-$ respectively. Candidate secondary decays, V^0, in the selected sample of hadronic events were found by considering all pairs of oppositely charged particles. The vertex defined by each such pair was determined such that the χ^2 of the hypothesis of a common vertex was minimized. The tracks were then refitted to the common vertex. The selection criteria were the "standard" ones described in [10]. The average detection efficiency from this procedure is about 36% for $K^0 \to \pi^+\pi^-$ and about 28% for $\Lambda \to p\pi^-$ in multihadronic events. The background under the invariant mass peaks was subtracted, separately for each bin of V^0 momentum, by linearly interpolating two sidebands in invariant mass which correspond to:

- the regions between 0.40 and 0.45 GeV/c^2 and between 0.55 and 0.60 GeV/c^2 for the K^0 ;
- the regions between 1.08 and 1.10 GeV/c^2 and between 1.14 and 1.18 GeV/c^2 for the Λ.

The procedure described above relies on the Monte Carlo simulation to obtain purity and efficiency of the particle identification. As a crosscheck also Z^0 events, taken at the beginning of the datataking period, were used to calibrate the detector performance. A matrix algorithm was then applied to unfold the observed rates. This method profits from the calibration of the detector performance on real data, but is difficult to apply to a low statistic sample. At energies of 130 and 183 GeV compatible results have been obtained.

4 Results

The ξ_p distribution after background subtraction was corrected bin by bin (for the detector acceptance and selection efficiency) using the simulation (JETSET). The corrected ξ_p

distributions for charged kaons, neutral kaons, protons and Λs at the various energies are shown in figure 1, figure 2, figure 3 and figure 4 respectively. In the figures the predictions from the generators JETSET 7.4 and HERWIG 5.8, and the fit to expression 3, are also shown. In the fit to the data distributions, s and k were fixed to the values obtained by fitting equation 3 to the corresponding JETSET 7.4 Monte Carlo distributions. Within the statistics of the data samples analysed, the shape of the ξ_p distribution is well described by both generators, JETSET 7.4 and HERWIG 5.8.

4.1 ξ^* distribution

The fit of the data points to expression 3 was used to extract the peak position of the ξ_p distribution, ξ^*.

In figure 5 and table 2 the results on the evolution of ξ^* with the centre of mass energy are presented. The data up to centre of mass energies of 91 GeV were taken from previous measurements [6]. The fit to expression 4, where F_h (Q_0) was taken as a free parameter and Λ_{eff} was fixed at 150 MeV (this value of Λ_{eff} comes from the description of the pion spectra with $\Lambda_{eff} = Q_0$, the limiting spectrum [2]), is superimposed to the data points (solid line). Figure 5 shows that (within the statistics of the data samples analysed) the fitted functions follow the data points rather well. This suggests that MLLA+LPHD gives a good description of the observed particle spectra.

From table 2 and figure 5 it is shown that there is good agreement between the data and the predictions from the generators JETSET 7.4 and HERWIG 5.8.

The systematic uncertainties on ξ^* were obtained as the sum in quadrature of the following contributions:

- From the original $dN/d\xi_p$ distribution two additional "distorted" distributions were obtained: one by adding 1 standard deviation to the values below ξ^* and subtracting 1 standard deviation to the values above, and the other by subtracting 1 standard deviation to the values below ξ^* and adding 1 standard deviation to the values above. From these distributions, two new values were obtained for ξ^*. These were compared to the values obtained from the normal distribution, and the larger difference was taken to be systematic uncertainty.

- The difference between the maximum using a distorted Gaussian fit and the maximum using a simple Gaussian fit.

The parameter Q_0 obtained from the fit (figure 5) is presented in table 3. It is observed that the Q_0 values obtained for the different particles are consistent within the uncertainty, although there is a systematic rise of Q_0 with the particle mass (apart from the proton results).

4.2 Average multiplicity

The multiplicity of the identified final states per hadronic event was obtained from the integration of the distributions shown in figures 1 to 4 inside a range varying according to the particle type and energy; outside this range the fraction of particles was extrapolated using the JETSET 7.4 prediction. The results are shown in figure 6 and table 4 and they

$\sqrt{s}$ (GeV)	Particle	Fitting range (GeV)	ξ^*		
			(Data)	JETSET 7.4	HERWIG 5.8
133	K^+	1.2-5.4	$2.95 \pm 0.06 \pm 0.13$	2.84	3.12
	K^0	0.6-5.4	$2.86 \pm 0.14 \pm 0.41$	2.87	3.15
	p	0.0-4.8	$2.92 \pm 0.08 \pm 0.14$	2.98	3.10
	Λ	0.6-4.8	$2.81 \pm 0.24 \pm 0.62$	2.79	2.99
161	K^+	1.2-4.8	$3.12 \pm 0.22 \pm 0.25$	2.96	3.25
	K^0	-	-	-	-
	p	1.2-4.8	$3.02 \pm 0.17 \pm 0.26$	3.08	3.23
	Λ	-	-	-	-
172	K^+	1.2-5.4	$3.10 \pm 0.09 \pm 0.37$	3.02	3.27
	K^0	-	-	-	-
	p	0.6-4.8	$3.17 \pm 0.11 \pm 0.82$	3.12	3.26
	Λ	-	-	-	-
183	K^+	1.2-5.4	$2.95 \pm 0.11 \pm 0.27$	3.01	3.30
	K^0	0.6-5.4	$3.08 \pm 0.15 \pm 0.30$	3.07	3.34
	p	0.6-4.8	$3.16 \pm 0.08 \pm 0.16$	3.15	3.30
	Λ	0.6-4.2	$2.84 \pm 0.14 \pm 0.38$	2.99	3.20
$WW \to q\bar{q}Q\bar{Q}$	K^+	1.3-5.4	$3.03 \pm 0.12 \pm 0.27$	3.38	-
	p	1.3-5.4	$3.33 \pm 0.20 \pm 0.43$	3.39	-
$WW \to q\bar{q}l\nu$	K^+	1.3-5.4	$3.40 \pm 0.25 \pm 0.60$	3.42	-
	p	1.3-5.4	$3.50 \pm 0.26 \pm 0.50$	3.41	-

Table 2: ξ^* $K^{\pm}$, K^0 , protons and Λ in hadronic events at 133 GeV, 161 GeV, 172 GeV and 183 GeV and WW events at 183 GeV. In the data the first uncertainty is statistical, the second is systematic.

Hadron	Q_0	χ^2
K^+	0.325 ± 0.009	2.5
K^0	0.330 ± 0.012	0.9
p	0.314 ± 0.011	0.5
Λ	0.343 ± 0.012	0.6

Table 3: Results of the fit of the evolution of ξ^* with the centre of mass energy.

$\sqrt{s}$ (GeV)	Particle	Integration range (GeV)	$< n >$ (Data)	JETSET 7.4	HERWIG 5.8
133	K^+	1.2-5.4	$2.58 \pm 0.10 \pm 0.13$	2.49	2.74
	K^0	0.6-5.4	$2.51 \pm 0.21 \pm 0.14$	2.40	2.64
	p	0.0-4.8	$1.25 \pm 0.08 \pm 0.03$	1.15	1.08
	Λ	0.6-4.8	$0.50 \pm 0.07 \pm 0.05$	0.34	0.49
161	K^+	1.2-4.8	$2.34 \pm 0.18 \pm 0.20$	2.63	2.90
	K^0	0.6-4.2	$2.56 \pm 0.38 \pm 0.25$	2.56	2.78
	p	1.2-4.8	$1.13 \pm 0.12 \pm 0.05$	1.25	1.19
	Λ	-	-	-	-
172	K^+	1.2-5.4	$2.95 \pm 0.23 \pm 0.17$	2.68	2.97
	K^0	-	-	-	-
	p	0.6-4.8	$1.41 \pm 0.17 \pm 0.04$	1.30	1.22
	Λ	-	-	-	-
183	K^+	1.2-5.4	$2.87 \pm 0.12 \pm 0.17$	2.74	3.02
	K^0	0.6-5.4	$2.09 \pm 0.18 \pm 0.16$	2.66	2.91
	p	0.6-4.8	$1.32 \pm 0.09 \pm 0.03$	1.33	1.24
	Λ	0.6-4.2	$0.42 \pm 0.06 \pm 0.09$	0.39	0.55
$WW \to q\bar{q}Q\bar{Q}$	K^+	1.3-5.4	$4.32 \pm 0.48 \pm 0.21$	4.04	-
	p	1.3-5.4	$2.22 \pm 0.51 \pm 0.06$	1.89	-
$WW \to q\bar{q}l\nu$	K^+	1.3-5.4	$1.79 \pm 0.41 \pm 0.11$	2.02	-
	p	1.3-5.4	$1.09 \pm 0.33 \pm 0.03$	0.94	-

Table 4: Average multiplicity for $K^{\pm}$, K^0 , protons and Λ for hadronic events at 133 GeV, 161 GeV, 172 GeV and 183 GeV and WW events at 183 GeV. In the data the first uncertainty is statistical, the second is systematic.

are compared with the predictions from JETSET 7.4 and HERWIG 5.8. In figure 6 the results shown for energies below 133 GeV (open squares) were extracted from [16].

The systematic uncertainties on the multiplicity were obtained as the sum in quadrature of the following contributions:

- The difference between the JETSET and HERWIG predictions in the unseen region.
- The uncertainty coming from the particle identification. A relative systematic uncertainty of 2% was estimated for protons and charged kaons (from the comparison between the standard and the tight NEWTAG selections), as applied in [17]. A relative uncertainty of 3% was estimated for K^0 [18] and 5% for Λ [19].
- For the W^+W^- sample the contribution due to the uncertainty in the QCD background was included.

The Monte Carlo programs JETSET 7.4 and HERWIG 5.8 display in general a fair agreement with the data. However the K^0 multiplicity at 183 GeV is 3.4 standard deviations (2.4 standard deviations) below the HERWIG (JETSET) predictions; HERWIG underestimates the results for protons at 133 GeV and overestimates the results for charged kaons at 161 GeV by 2 standard deviations.

5 Conclusions

The production of K^+ , K^0 , p and Λ at centre-of-mass energies above the Z^0 peak has been studied using data taken with the DELPHI detector at LEP. The results on the average multiplicity of such identified particles and on the position ξ^* of the maximum of the $\xi_p = -\log(\frac{2p}{\sqrt{s}})$ distribution have been compared with predictions of JETSET and HERWIG, and with calculations based on MLLA+LPHD approximations.

The Monte Carlo programs JETSET 7.4 and HERWIG 5.8 display in general a fair agreement with the data. However the measured K^0 multiplicity at 183 GeV is 3.4 standard deviations (2.4 standard deviations) below the HERWIG (JETSET) predictions; HERWIG underestimates the results for protons at 133 GeV and overestimates the results for charged kaons at 161 GeV by 2 standard deviations.

For the W^+W^- sample the available statistic is small. A fair agreement with the prediction of the generator has been found in both multiplicities and ξ^*.

Within the statistics of the data samples analysed the shape of the ξ_p distribution is well described by both generators, JETSET and HERWIG. The parameter Q_0 was estimated. It is observed that the Q_0 values obtained for the different particles are consistent within the uncertainties, although there is a systematic rise of Q_0 with the particle mass (excluding the proton results).

Acknowledgements

We are greatly indebted to our technical collaborators and to the funding agencies for their support in building and operating the DELPHI detector. Very special thanks are due to the members of the CERN-SL Division for the excellent performance of the LEP collider. We are grateful to V. Khoze for useful discussions.

References

[1] V.A. Khoze and W. Ochs, Int. J. Mod. Phys. **A12** (1997) 2949.

[2] Y.I. Azimov et al., Z. Phys. **C27** (1985) 65 and ibid. **C31** (1986) 213.

[3] A.H. Mueller, in Proc. 1981 Intern. Symp. on Lepton and Photon Interactions at High Energies ed. W.Pfeil (Bonn 1981) 689;
Yu.L. Dokshitzer, V.S.Fadin and V.A. Khoze, Phys. Lett. B 115 (1982) 242.

[4] Yu.L. Dokshitzer, V.A. Khoze and S.I. Troyan, Int. J. Mod. Phys. **A7** (1992) 1875.

[5] C.P. Fong and B.R. Webber, Phys. Lett. **B229** (1989) 289.

[6] N.C.Brummer, Z. Phys. **C66** (1995) 367.

[7] T. Sjöstrand, Comp. Phys. Comm. **82** (1994) 74.

[8] G. Marchesini and B.Webber, Nucl. Phys. **B310** (1988) 461;
G. Marchesini et al., Comp. Phys. Comm. **67** (1992) 465.

[9] DELPHI Coll., P. Abreu et al., Nucl. Instr. Methods **A303** (1991) 233.

[10] DELPHI Coll., P. Abreu et al., Nucl. Instr. Methods **A378** (1996) 57.

[11] DELPHI Coll., P. Abreu et al., Z. Phys. **C77** (1996) 11.

[12] DELPHI Coll., P. Abreu et al., Phys. Lett. **B372** (1996) 172.

[13] S. Bethke et al., Nucl. Phys. **B370** (1992) 310.

[14] P. Buschman et al.,"Measurement of W-pair Production cross-section at $\sqrt{s}$=183 GeV", DELPHI note 98-20 CONF 120.

[15] E.Schyns, "NEWTAG, $\pi^{\pm}$, $K^{\pm}$ and $p\bar{p}$ tagging for DELPHI RICHes", DELPHI note 96-103 RICH-89.

[16] Review of Particle Properties 1994, Particle Data Group, Phys. Rev. **D50** n.3 (1994) 1173.

[17] DELPHI Collab., E. Schyns, DELPHI note 97-110 CONF 92, contribution n. 541 to the Jerusalem Conference on HEP (1997).

[18] DELPHI Collab., P. Abreu *et al.*, Z. Phys. **C65** (1995) 587.

[19] DELPHI Collab., P. Abreu *et al.*, Phys. Lett. **B318** (1993) 249.

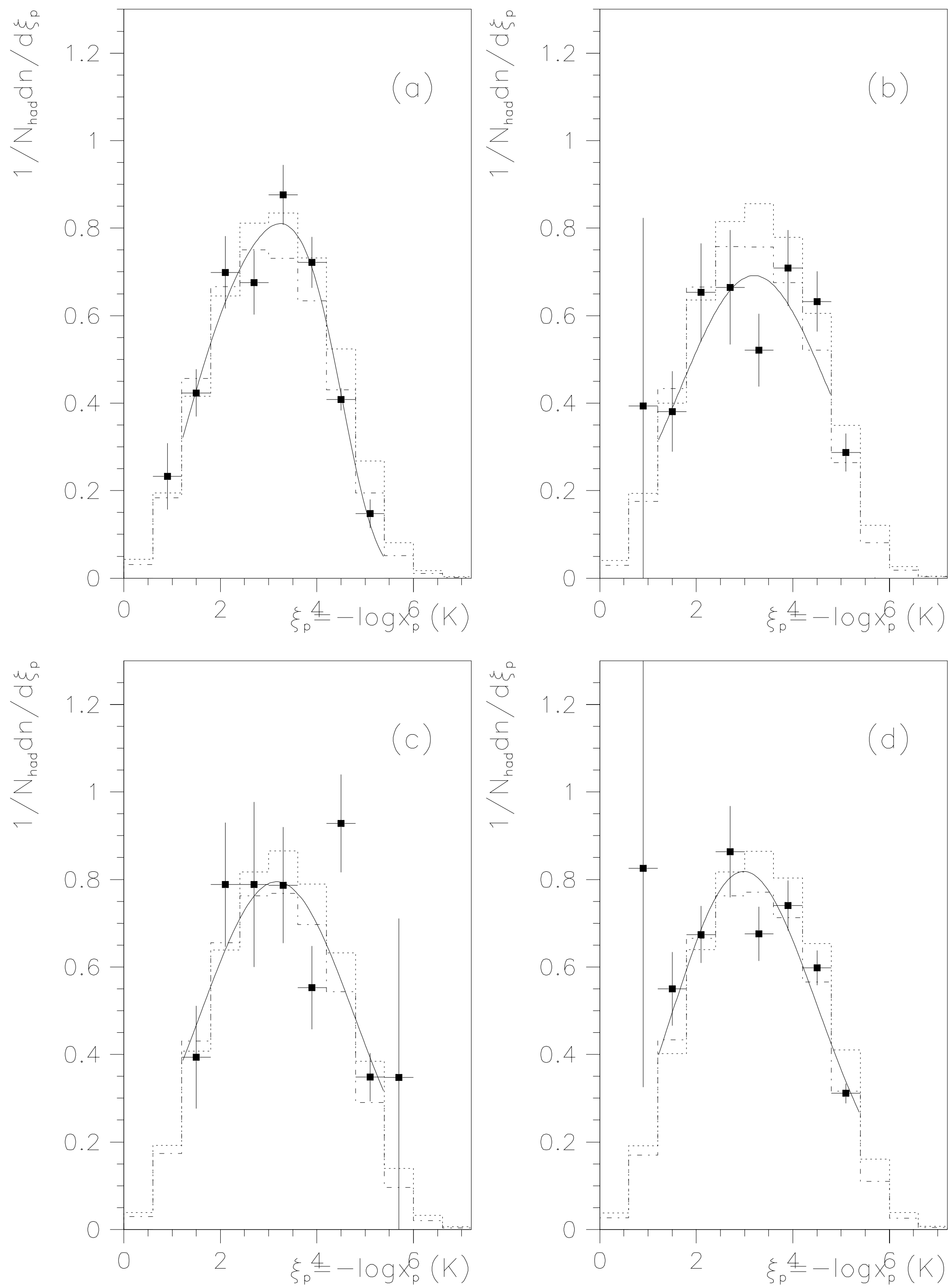

Figure 1: ξ_p distributions (efficiency corrected) for charged kaons at 133 GeV/c (a), 161 GeV/c (b), 172 GeV/c (c) and 183 GeV/c (d): data (points), simulation using JETSET (dashed-dotted line) and HERWIG (dotted line). The full curves show the fit of the data to the distorted Gaussian.

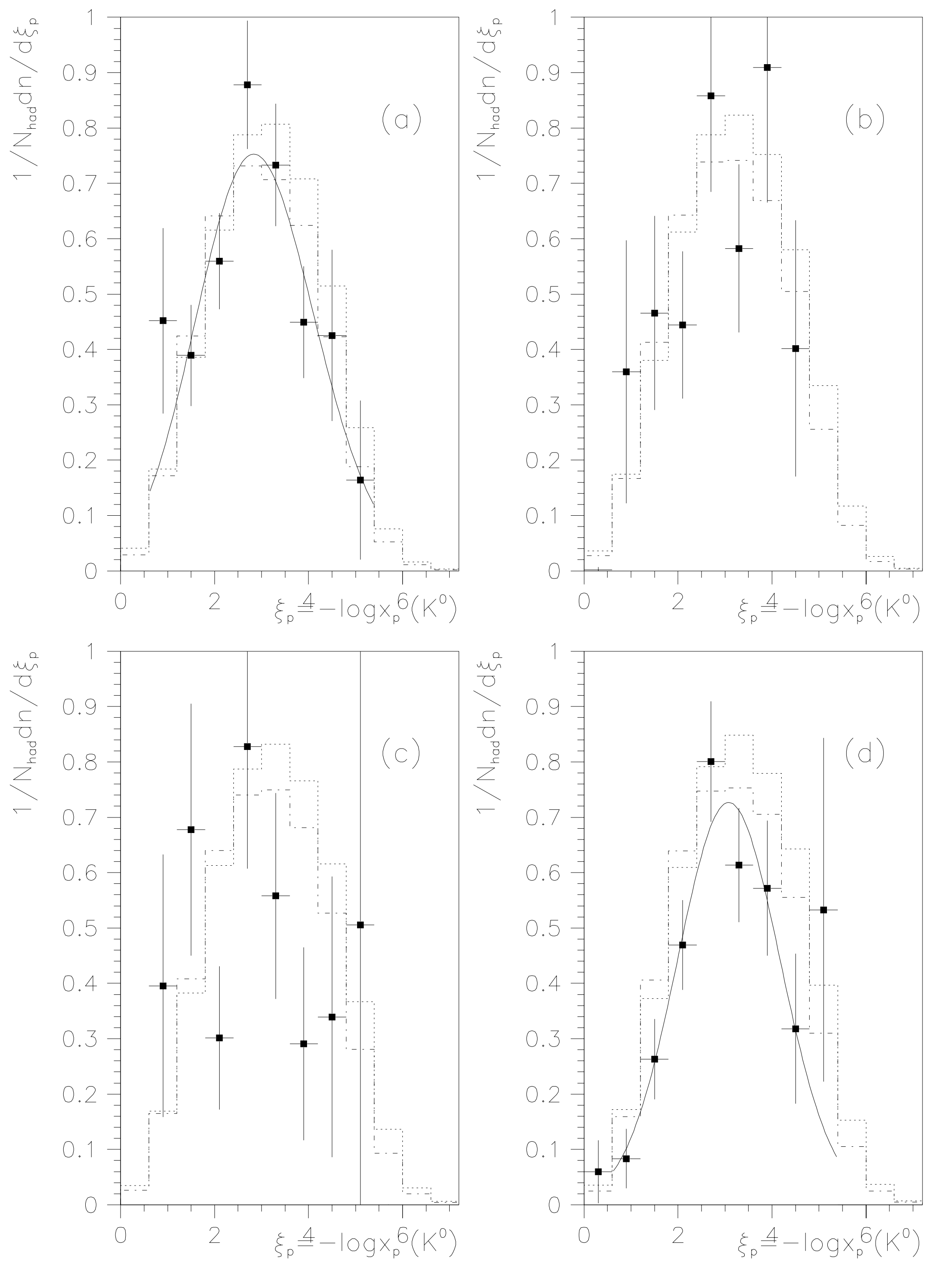

Figure 2: ξ_p distributions (efficiency corrected) for neutral kaons at 133 GeV/c (a), 161 GeV/c (b), 172 GeV/c (c) and 183 GeV/c (d): data (points), simulation using JETSET (dashed-dotted line) and HERWIG (dotted line). The full curves show the fit of the data to the distorted Gaussian.

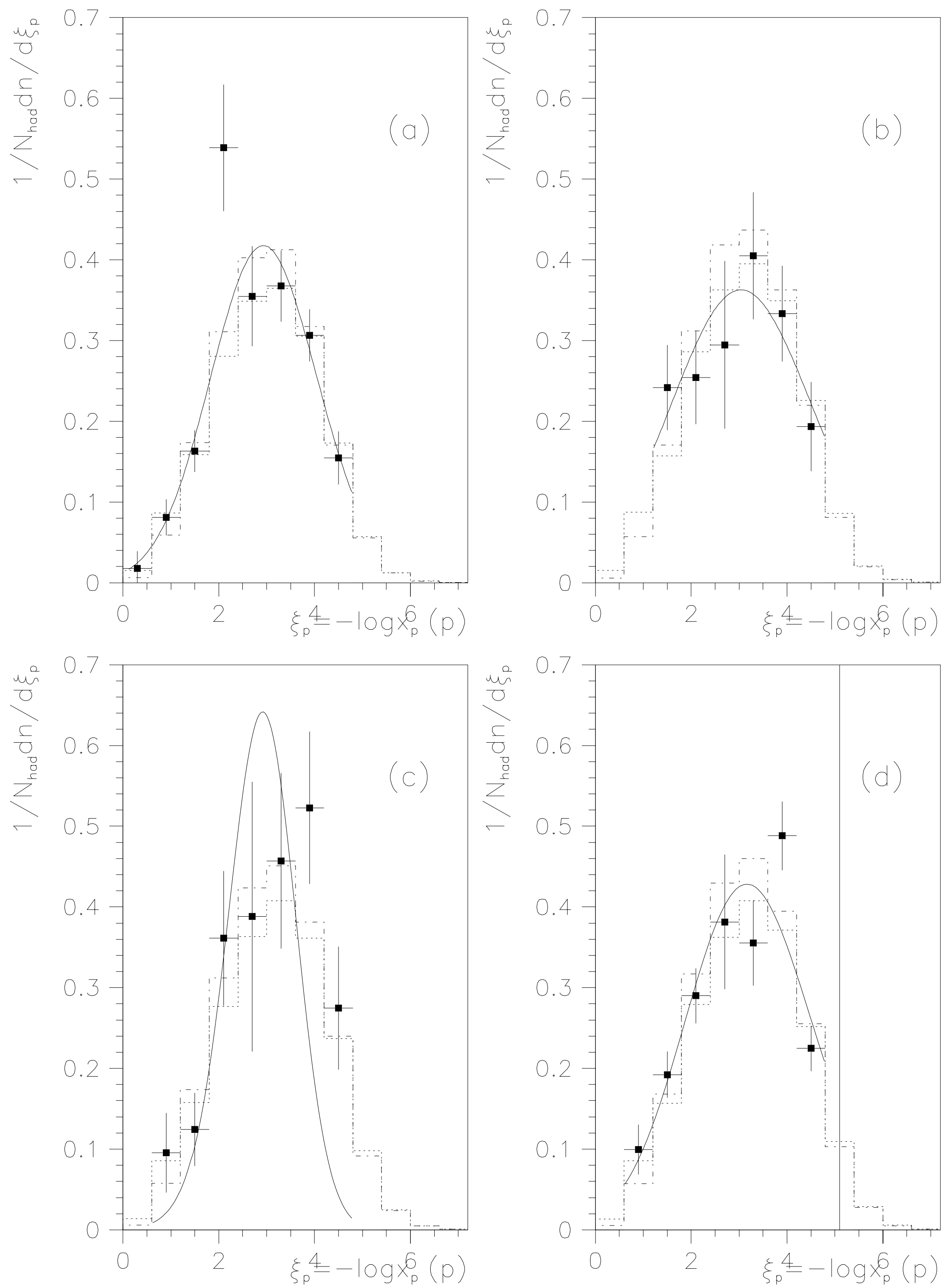

Figure 3: ξ_p distributions (efficiency corrected) for protons at 133 GeV/c (a), 161 GeV/c (b), 172 GeV/c (c) and 183 GeV/c (d): data (points), simulation using JETSET (dashed-dotted line) and HERWIG (dotted line). The full curves show the fit of the data to the distorted Gaussian.

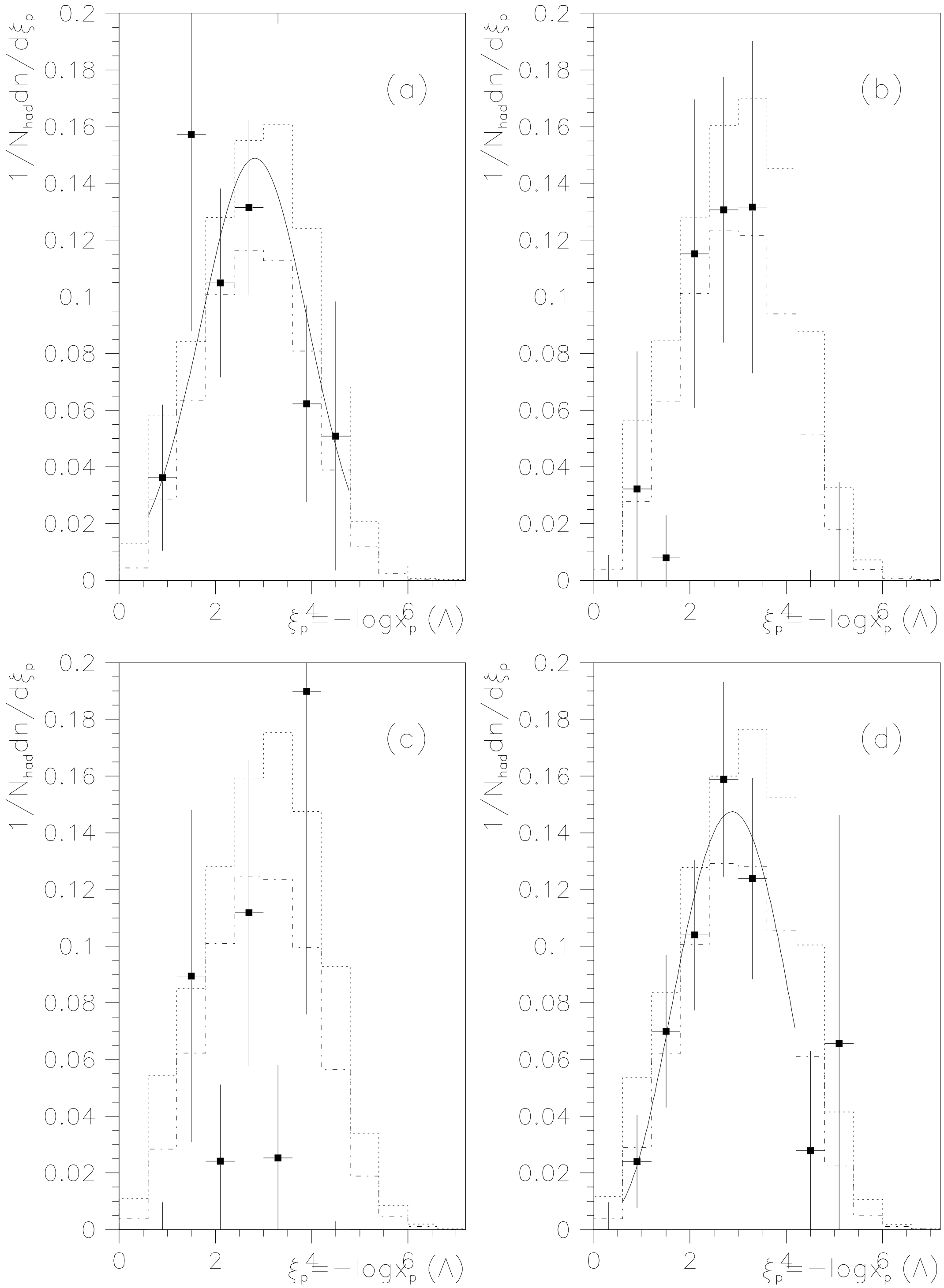

Figure 4: ξ_p distributions (efficiency corrected) for Λ at 133 GeV/c (a), 161 GeV/c (b), 172 GeV/c (c) and 183 GeV/c (d): data (points), simulation using JETSET (dashed-dotted line) and HERWIG (dotted line). The full curves show the fit of the data to the distorted Gaussian.

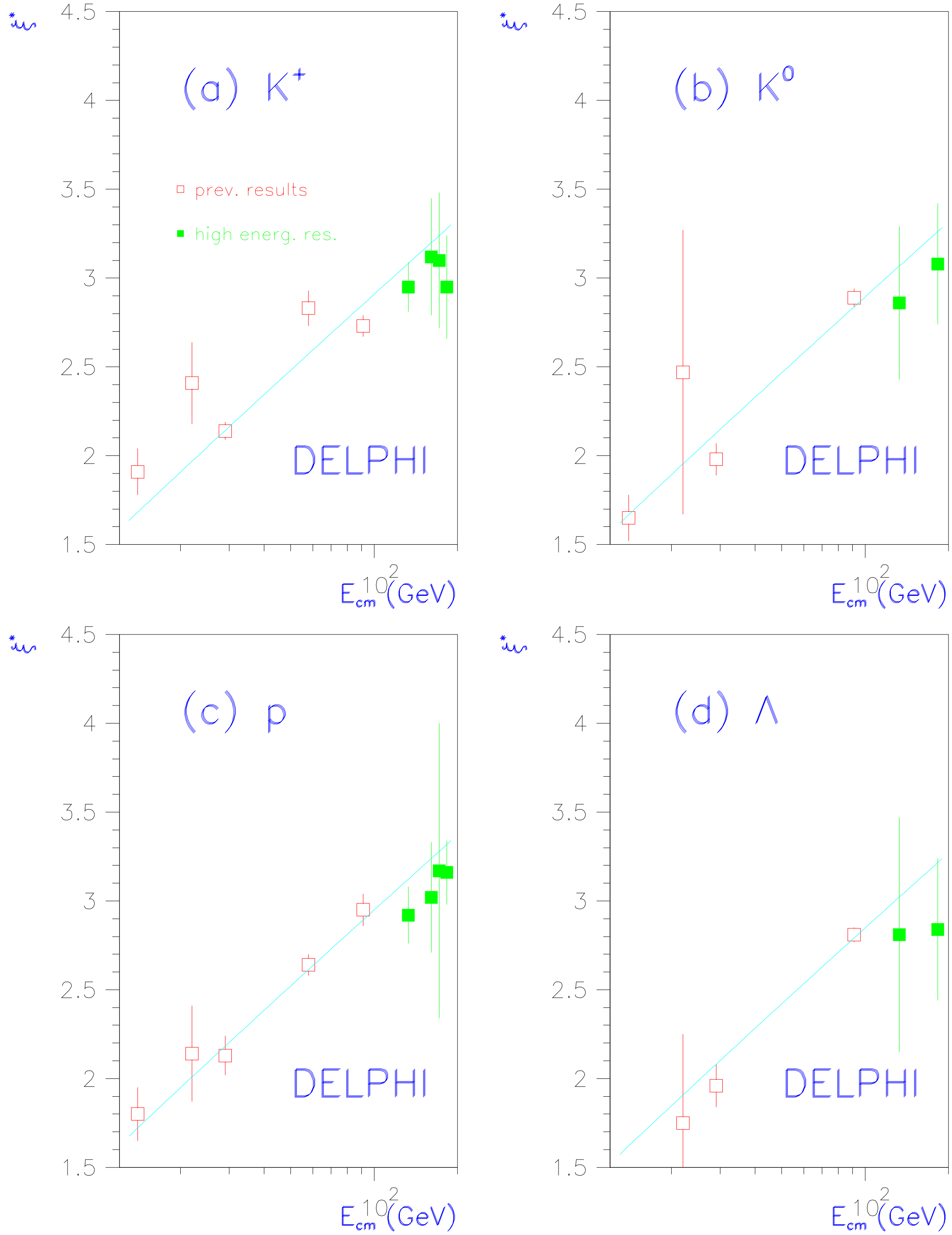

Figure 5: The maximum ξ^* of the ξ_p-distribution is shown for K^+ (a), K^0 (b), p (c) and Λ (d) as function of the centre-of-mass energy (closed squares). The fit (solid line) is superimposed to the data points (see text).

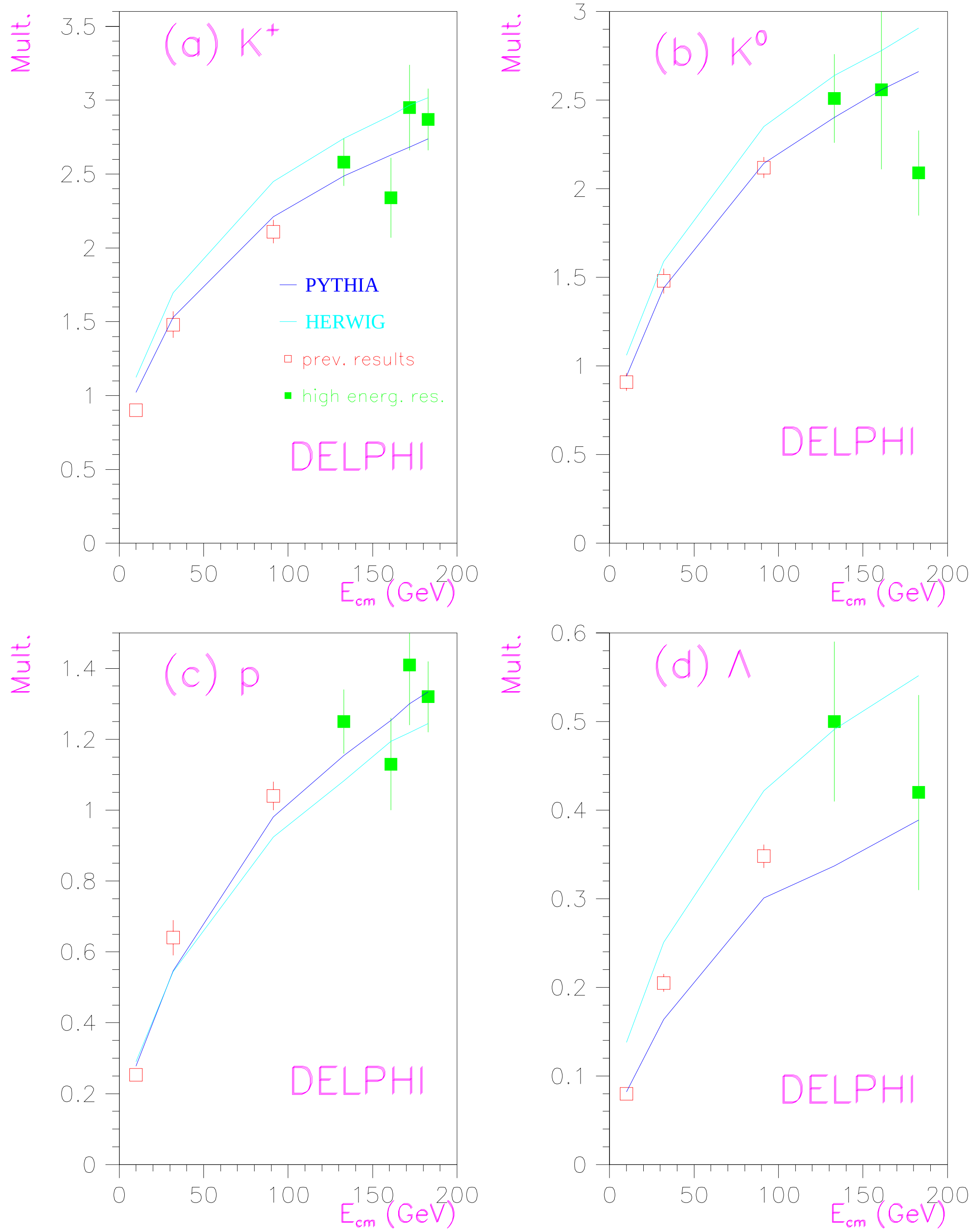

Figure 6: Average multiplicity of K^+ (a), K^0 (b), p (c) and Λ (d) as function of the centre-of-mass energy (black squares). Simulation using JETSET 7.4 (open circles) and HERWIG 5.8 (open crosses) are superimposed.